Journal of The Electrochemical Society, **158** (4) C95-C103 (2011)
0013-4651/2011/158(4)/C95/9/$28.00 © The Electrochemical Society

Evaluation of 316L Stainless Steel Corrosion Resistance in Solution Simulating the Acid Hydrolysis of Biomass

E. A. Ferreira, R. D. Noce, C. S. Fugivara, and A. V. Benedetti[*,z]

Departamento de Físico-Química, Instituto de Química, Universidade Estadual Paulista, UNESP, 14801-970 Araraquara, São Paulo, Brazil

The corrosion resistance of 316L stainless steel in 65 wt % ethanol, 35 wt % water, 1 wt % H_2SO_4 solution containing different NaCl concentrations and at different temperatures was investigated using open circuit potential measurements, polarization curves, and electrochemical impedance spectroscopy. At 25°C, the minimum NaCl concentration required for occurrence of pitting was 0.58 wt %. In 0.35 wt % NaCl solution, localized corrosion was observed at temperatures higher than 40°C and, depending on the potential, metastable or stable pits were observed. No pits were observed below 40°C in 0.35 wt % NaCl solution.
© 2011 The Electrochemical Society. [DOI: 10.1149/1.3554728] All rights reserved.

Manuscript submitted September 2, 2010; revised manuscript received December 14, 2010. Published February 28, 2011.

Stainless steels are used as construction materials for key corrosion-resistant equipment in most of the major industries, and especially in chemical, petroleum, processing, and power generation plants. A very thin film, known as the passive film, which is self-healing in a wide variety of environments,[1–4] provides their corrosion resistance. Due to environmental concerns, there has recently been an increase in the demand for ethanol as a road vehicle fuel. There is therefore, a greater need for studies of the corrosion resistance of materials used in alcohol production plants, and in transportation and storage facilities.

Among these stainless steels, the 300 series stands out. The 300 series represents compositional modifications of the classic 18/8 (18% Cr–8% Ni) stainless steel, which has been a popular corrosion-resistant material for some 70 years, to improve pitting, crevice and stress corrosion resistance, high-temperature oxidation resistance and strength, and reduce intergranular corrosion in welded materials. Type 304 is the general-purpose grade, widely used in applications requiring a good combination of corrosion resistance and formability. On the other hand, type 316 contains molybdenum and has greater resistance than type 304 to pitting in marine and chemical industry environments.[1]

Electrochemical corrosion causes between $8 billion and $128 billion in economic damage per year in the United States alone,[5] and pitting corrosion constitutes one of the most important failure mechanisms. Pits cause failure through perforation, and engender stress corrosion cracks.[1] Pitting corrosion has been studied for the last few decades and, according to Frankel,[6] fundamental studies have focused on characterization of the passive film, the initial stages of passive film breakdown, metastable pitting growth, and the growth of large and stable pits.

Solution chloride concentration is a very important parameter influencing pitting formation on stainless steels. Increasing the chloride concentration significantly increases the possibility of pitting. The chloride levels that can be tolerated without the onset of pitting increase with the chromium and molybdenum contents of austenitic and ferritic stainless steels (for example, the minimum chloride ion concentration in 1 mol L^{-1} H_2SO_4 for initiation of pitting on pure Fe is 0.3 mmol L^{-1}, while on Fe-18.6Cr-9.9Ni alloy it is 0.1 mol L^{-1}).[1]

Electrochemical studies of pitting corrosion have found the existence characteristic potentials. Stable pits form at potentials noble to the pitting potential, E_p, and will grow at potentials nobler than the repassivation one, E_R, which is lower than E_p. During upward scanning in a cyclic polarization experiment, a stable pit starts growing at E_p, where the current increases sharply from the passive current level and, upon reversal of the scan direction, repassivates at E_R where the current drops back. It is generally considered that materials exhibiting higher values of E_p and E_R are more resistant to pitting corrosion, and cyclic polarization experiments are commonly used for this purpose.[6,7] A correlation has been found such that metals with low experimentally determined pitting potential have a higher tendency to form pits naturally at open circuit. E_p is in many cases a function of experimental parameters such as potential scan rate. Furthermore, so-called metastable pits initiate and grow for a period at potentials well below the pitting potential, which provides evidence in contradiction to the definition of the pitting potential as being the potential above which pits initiate. Metastable pits initiate and grow for a limited period before repassivating. Large pits can stop growing for several reasons, but metastable pits are typically considered to be those of micron size at most, with lifetimes on the order of seconds or less.[6]

Temperature is also a critical factor in pitting corrosion since many materials will not pit at a temperature below a certain value, which may be extremely sharp and reproducible. This effect can be seen either by varying the temperature at a range of fixed applied potentials, or by varying the potential for a range of constant temperature. At low temperatures, extremely high breakdown potentials are observed, corresponding to transpassive dissolution, rather than localized corrosion. Just above the critical pitting temperature (CPT), pitting corrosion occurs at a potential that is far below the transpassive breakdown potential.[6] Laycock et al.[8] showed that at the critical pitting temperature for 904L stainless steel, the maximum amount of metastable pit formation occurred about 300 mV versus SCE. The morphology of these pits was examined by SEM, and a model was proposed considering the precipitation of a $FeCl_2$ film inside the pits as being the critical point; above the CPT, this film is essential for the growth of stable pits. The metastable pits most likely grow with no salt film and repassivate by virtue of the violent rupture of the pitting covering, that dissolves the media in which the pit has been formed. Conditions, for example, temperature increase, favour formation a salt film, there is a high probability of the pitting resisting rupture of covering, producing a stable pit due to the buffering action of the salt, renewing the pitting medium by dissolution.[6]

Stainless steels, for example types 304 and 316, contain a variety of inclusions such as oxides, silicates, aluminates, and sulphides. These inclusions are often mixed, with the sulphides forming shells around the oxides, silicates and aluminates. The manganese sulphide shell is a particularly favourable location for pit initiation.[9,10]

Refaey et al.[11] reported on corrosion studies using polarization curves from −0.7 to 2 V(Ag/AgCl/KClsat), at 20 mV s^{-1}, for 316L stainless steel in different concentrations of NaCl solution (0.01–2.0 mol L^{-1}). They observed that the NaCl concentration did not affect the shape of the curves, which were characterized by the appearance of passive and transpassive regions. It was also noticed that the current increased suddenly, without any sign of oxygen evolution, indicating the breakdown of the passive layer and pitting corrosion nucleation.

When 316L stainless steel was exposed to either aqueous solution or a mixture of 35 wt % water and 65 wt % ethanol, both

* Electrochemical Society Active Member.
z E-mail: benedeti@iq.unesp.br

Downloaded on 2013-07-18 to IP 186.217.234.138 address. Redistribution subject to ECS license or copyright; see ecsdl.org/site/terms_use

containing 1 wt % H_2SO_4 and 0.35 wt % NaCl, it was shown that the presence of ethanol inhibited steel dissolution, as evidenced by an increase in the corrosion potential.[12] In solution consisting of the ethanol-water mixture (without acid) and 1.70 wt % NaCl, the corrosion and pitting potentials were similar to those obtained in aqueous solution. The oxide film formed potentiodynamically on the electrode surface presented similar resistivity in both aqueous solutions and ethanol-water mixture containing 1.70 wt % NaCl.[12]

According to Anna,[13] corrosion-protection principles, as they are known from corrosion in aqueous solutions, are not applicable in solving materials problems; organic solvents differ from aqueous ones in their physicochemical and chemical properties. Sekine et al.[14] studied the corrosion behaviour of stainless steel in aqueous ethanol solution containing sulphuric acid. These authors showed that the corrosion rate increased with decrease of EtOH concentration and increase of Cr content. It is believed that susceptibility to corrosion is promoted because both the conductivity of the solution and the charge transfer increase. In contrast, as the concentration of EtOH increases, the corrosion reaction is suppressed by an additive property based on both the increase of the corrosion resistance and the formation of the stable passive film.

The corrosion studies found in the literature describing the behaviour of stainless steels in alcoholic solutions and alcohol/water mixtures mostly concern the 300 series steels, especially the 304 steels.[15–20] Studies concerning 316 steels have focused on solutions containing anhydrous methanol and LiCl at high temperatures and pressures.[21,22]

The augment of ethanol production with no enlargement of plantation area occurs by means of hydrolysis system of the bagasse and straw of sugarcane. The hydrolysis process of the bagasse is made from the ethanol/water mixture as solvent and sulphuric acid at temperatures ranging from 170 to 185°C.[23] To develop it is mandatory the use of metallic materials that undergo high pressures and temperatures. However, these materials may be corroded owing to high temperatures, presence of abrasives, and existence of chloride coming from the systems of water distribution, the own sugarcane bagasse and/or residues.

The use of these materials in industrial systems, including ethanol plants, is of great interest. However, systematic studies of corrosion of 316L stainless steels in solutions comprising ethanol/water/NaCl mixtures are lacking in the literature. Therefore, the objective of this work was to evaluate 316L stainless steel corrosion resistance in ethanol (65 wt %)/water (35 wt %)/H_2SO_4 (1 wt %) solutions containing different NaCl concentrations, and at different temperatures, using open circuit potential measurements, polarization curves and electrochemical impedance spectroscopy. This manuscript addresses the susceptibility of 316L stainless steel to corrosion under relatively severe conditions, similar to those used in the acid hydrolysis of bagasse.

Materials and Methods

Sample preparation.— The working electrode was a 316L stainless steel (SS), kindly provided by DEDINE S.A., and according to the ASTM, the nominal composition of this kind of steel is (wt %) 16–18 (Cr), 10–14 (Ni), 0.03 (C), 2.0 (Mn), 1.0 (Si), 0.045 (P), 0.03 (S), 2–3 (Mo).[1] A geometrical area of 1 cm^2, delimited by an O-ring, was exposed to the electrolyte. When an O-ring for assembly of working electrode is used there is the possibility of having crevice. No crevice was observed when the potential was swept up to around 0.1 V higher than the pitting one and/or if it was held at the pitting potential (or at slightly higher values) for less than 1 min. At these conditions the number and size of pits increased. When the electrodes were polarized at potentials higher than the pitting one for more than 1 min, pits and crevice were observed near the O-ring.

The electrode surface (2 cm length × 1.5 cm width × 2 mm thickness) was progressively polished, starting with 600 and 1200 grade emery papers, and finishing with a 1 μm diamond suspension, using a polisher (BUEHLER). The electrodes were then washed and sonicated with acetone in an ultrasonic bath for 10 min, dried using oil-free compressed air, and immediately introduced into the electrochemical cell.

Electrochemical cell and equipment.— All electrochemical studies were carried out in a Tait type conventional three-electrode electrochemical cell. The counter electrode was a Pt network, and all potentials were measured and referred to an aqueous $Ag/AgCl/KCl_{sat}$ reference electrode connected to the working solution through a Luggin capillary. For all electrochemical measurements a saturated KCl solution was placed inside the Luggin capillary, therefore no significant liquid junction potentials are expected. At the end of the capillary a titania ceramic piece was welded. Therefore, the ionic contact was done by microcracks formed due to the different thermal expansion coefficient between the ceramic and glass. To investigate a possible chloride contamination of the working solution by chloride coming from the the Luggin some tests were done. For the test, the reference electrode was placed inside the Luggin capillary containing saturated KCl solution, and the working solution without chloride ions inside the electrochemical cell. After 2 h (the mean experimental time) 1 g of silver nitrate was added to the water and no precipitation or cloudiness was detected. On the contrary, when silver nitrate was added, for instance, to a 65 wt % ethanol, 35 wt % water, 1 wt % H_2SO_4 and 6×10^{-5} wt % NaCl solution, the more diluted one, precipitates or cloudiness was observed. Therefore, it was concluded that the contamination of the working solution with chloride from the reference electrode did not occur or was not significant. Another evidence that no significant chloride leakage occurred can be inferred from the open circuit potential measurements during 5 h in the working solution, since the open circuit potential, after some immersion time, did not change with time, and was dependent on the Cl^- concentration in the working solution.

Polarization curves (PC) and electrochemical impedance (EIS) measurements were performed using an EG & G potentiostat (Model 273 A) and a Solartron-SI1255 system.

Electrochemical procedure.— Electrochemical experiments were performed in aerated and unstirred 65 wt % ethanol, 35 wt % water, 1 wt % H_2SO_4 solution, with different NaCl concentrations, at different temperatures and *p*H 0.6 (Table I). The solutions were prepared from analytical grade reagents and Milli-Q water (18.2 MΩ cm). Before measuring the polarization curves, the electrode was immersed in the working solutions for 2 min or 5 h. Finally, the anodic potential scan was performed at 0.167 mV s^{-1}, starting at −50 mV($Ag/AgCl/KCl_{sat.}$)/E_{OCP} (open circuit potential) and scanning towards positive potential, either until the appearance of localized corrosion or until the transpassive region was reached. The electrochemical impedance spectroscopy (EIS) measurements were carried out after exposing the steel to the electrolyte for different time intervals. The impedance experiments were performed over a frequency range of 100 kHz to 5 mHz, with a potential sine wave amplitude of 10 mV (rms) and 10 points/decade at 25°C.

Ethanol influence on the potential of the aqueous acid-NaCl-containing solution and liquid junction potential values at the aqueous/ethanolic interface.— The effect of ethanol was estimated based on the potential difference measured for at least 18 min using the electrochemical cells shown in 1 and 2. The salt bridge was

Table I. Electrochemical techniques, chloride concentration and temperature used in the corrosion study of 316 L stainless steel in 65 wt % ethanol, 35 wt % water, 1 wt % H_2SO_4 solution.

Electrochemical technique	Chloride concentration (wt %)	Temperature (°C)
OCP	6×10^{-5} and 6×10^{-3}	25
CP	6×10^{-5} to 0.58	25
	0.35	25–80
EIS	6×10^{-5}	25

Downloaded on 2013-07-18 to IP 186.217.234.138 address. Redistribution subject to ECS license or copyright; see ecsdl.org/site/terms_use

composed of a tube in U form filled with 3 mol L^{-1} KCl aqueous solution

$$Ag/AgCl/KCl_{sat.}//65\ wt\ \%\ ethanol,\ 35\ wt\ \%\ H_2O,\ 1\ wt\ \%\ H_2SO_4,\ x\ wt\ \%\ NaCl/Ag/AgCl/KCl_{sat} \quad [1]$$

and

$$Ag/AgCl/KCl_{sat.}//\ H_2O,\ 1\ wt\ \%\ H_2SO_4,\ x\ wt\ \%\ NaCl/Ag/AgCl/KCl_{sat} \quad [2]$$

where x was 6×10^{-5}, 2×10^{-2} and 0.58 wt % NaCl, respectively.

The potential difference between these two electrochemical cells (1) and (2) are listed in Table II for different NaCl concentration. An excess of AgCl was added to the ethanolic acid solution to avoid the effect of ethanol and sulfate ion on the possible AgCl film dissolution. The difference between the potential values of these two electrochemical cells for a constant NaCl concentration (48 ± 3 mV/Ag/AgCl/$KCl_{sat.}$) represents the ethanol influence in the potentials measured in this system, mainly due to the difference of the chloride ion activity in both solutions, considering that no influence of junction potential should be present. In the conditions of the present work, this potential difference was independent of the NaCl concentration.

An estimative of the liquid junction potential was obtained based on the measurement of the potential difference between cells (3) and (1)

$$Ag/AgCl/KCl_{sat.}/65\ wt\ \%\ ethanol,\ 35\ wt\ \%\ H_2O,\ 1\ wt\ \%\ H_2SO_4,\ 0.006\ wt\ \%\ NaCl/Ag/AgCl/KCl_{sat.} \quad [3]$$

$$Ag/AgCl/KCl_{sat.}//65\ wt\ \%\ ethanol,\ 35\ wt\ \%\ H_2O,\ 1\ wt\ \%\ H_2SO_4,\ 0.006\ wt\ \%\ NaCl/Ag/AgCl/KCl_{sat.} \quad [4]$$

As the NaCl concentration increases the potential values of electrochemical cells (3) and (1) decreases due to the increase in the chloride ion activity. The junction potential values increases negatively in the ethanolic solutions and decreases in aqueous ones, suggesting that the ion chloride (and also the sulfate ion) mean activity coefficient is more influenced in ethanol than in aqueous solutions, probably owing to the decrease of the salt solubility in ethanol.

Scanning electron microscopy (SEM) analysis.— SEM micrographs of the electrode surface were taken using a scanning electron microscope (JEOL T330A), after scanning up to different potentials under varying conditions of chloride concentration and temperature. The inclusions were observed using a scanning electron microscope with Field Emission Gun (PHILIPS XL30FEG) coupled to the energy dispersive (EDS) microanalysis system (Oxford Instruments). The microanalyses were performed using 25 kV, and with 100 s acquisition time.

Results and Discussion

Open circuit potential and potentiodynamic polarization.— Figure 1 shows the open circuit potential (E_{OC}) versus time for

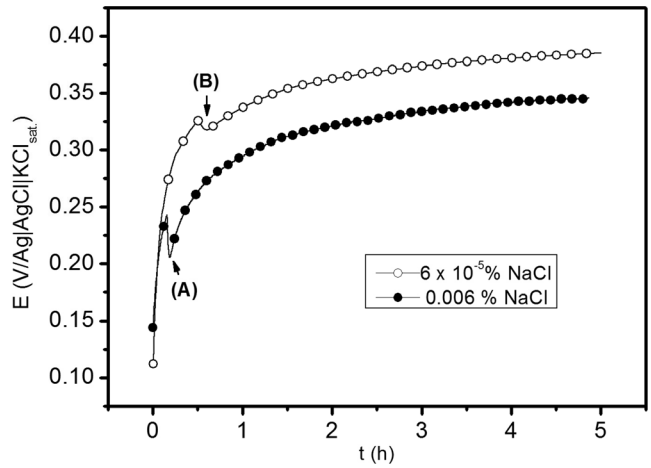

Figure 1. Open circuit potential values for 316L stainless steel in 65 wt % ethanol, 35 wt % water, 1 wt % H_2SO_4 solution containing different NaCl concentrations, at 25°C.

316L stainless steel in 65 wt % ethanol, 35 wt % H_2O, 1 wt % H_2SO_4 solutions containing 6×10^{-5} wt % and 0.006 wt % NaCl. The open circuit potential increased fast during the first 25 and 10 min for the solutions containing 6×10^{-5} wt % and 0.006 wt % NaCl, respectively. At these times a discontinuity of potential was observed and afterwards the potential continued increasing exponentially to about 2 h, and therefore only a monotonic potential increase was noticed for both E-t curves. After 5 h of immersion in solutions containing 6×10^{-5} wt % and 0.006 wt % NaCl the open circuit potential values were around 0.37 and 0.33 V(Ag/AgCl/$KCl_{sat.}$), respectively. This increase of potential indicates that a protective oxide was formed on the metal surface.

Both Cr and Ni influence the open circuit potential of the stainless steel since they can form metallic oxides when immersed in aqueous solutions, which cause the open circuit potential increase, mainly in the initial immersion times. Studies performed by P. Brüesch et al.[24] showed that open circuit potential of chromium increases with time when immersed in 0.1 mol L^{-1} NaCl aqueous solution, reaching an almost constant value of −0.175 V/(Ag/AgCl/$KCl_{sat.}$). The open circuit potential for Ni also increased with time when immersed in 0.1 mol L^{-1} KCl aqueous solution and stabilizes close to −0.130 V/(Ag/AgCl/$KCl_{sat.}$) after around 30 min of immersion.[25] This increase is associated with the oxide film thickening, and is also related to the nature of the oxide film which may be altered by the incorporation of species from the electrolyte.[26–29] In addition, El Kader and El Din[25] also noticed that for KCl concentrations higher than 1×10^{-2} mol L^{-1} there was a decrease of E_{oc} (after reaching the steady state potential) with increasing KCl concentration. Both results indicate the oxide formation on Cr and Ni. Considering the 316L stainless steel, the open circuit potential, for instance, around −0.34 V/(Ag/AgCl/$KCl_{sat.}$) in 65 wt % ethanol, 35 wt % water, 1 wt % H_2SO_4 solution containing 0.006 wt % NaCl, at 25°C, is higher than pure Cr and Ni, indicating

Table II. Potential values for cells with and without junction potential, junction potential value and potential attributed to the influence of ethanol.

Solution*	[Cl^-]/wt%	E_{Cell} (3)/mV	E_{Cell} (1)/mV	E_j = E(3)-E(1)/mV	$E_{ethanol}$ = E(1)-E(2)/mV
Ethanolic (a)	6×10^{-5}	202	202	0	51 (a1–b1)
Aqueous (b)	6×10^{-5}	231	151	80	
Ethanolic (c)	2×10^{-2}	143	162	–19	47 (c1–d1)
Aqueous (d)	2×10^{-2}	159	115	44	
Ethanolic (e)	0.58	54	83	–29	46 (e1–f1)
Aqueous (f)	0.58	89	37	52	

* All solutions contain 1 wt% H_2SO_4. The ethanolic solutions contain 35 wt% water.

Downloaded on 2013-07-18 to IP 186.217.234.138 address. Redistribution subject to ECS license or copyright; see ecsdl.org/site/terms_use

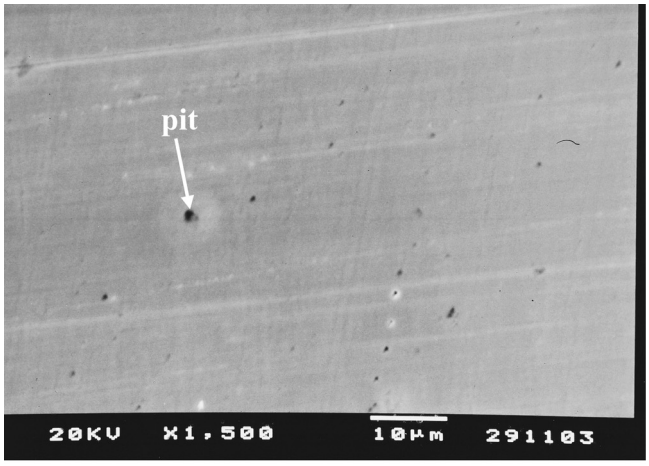

(A)

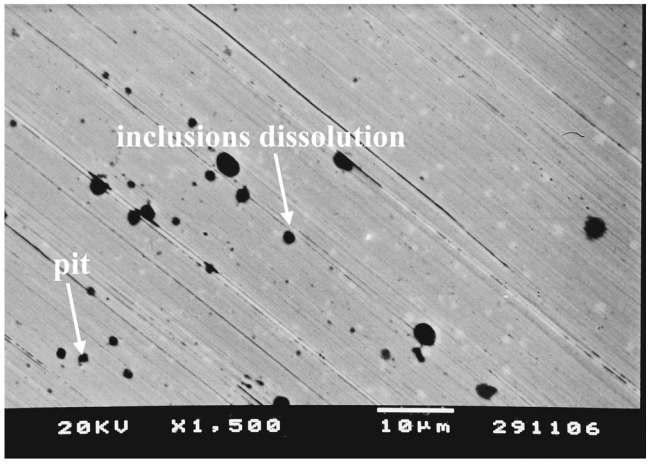

(B)

Figure 2. SEM images of polished 316L stainless steel after 20 (A) and 30 (B) min of immersion in 65 wt % ethanol, 35 wt % water, 1 wt % H_2SO_4 solution containing 0.006 wt % NaCl, at 25°C.

the strong influence of these elements on the behavior of the alloy. When the chloride concentration increased the open circuit potential decreased because of the attack to the oxide passive film generates defects, and also due to the chloride adsorption on the electrode surface.

A discontinuity was also noticed in both E_{OC} *vs*. time curves, after ~10 min immersion in the solution containing 0.006 wt % NaCl, and after ~25 min immersion in the solution containing 6×10^{-5} wt % NaCl, at 25°C. This discontinuity is well-reproducible and it might be associated with the dissolution of superficial MnS inclusions present in the steel. The dissolution of inclusions exposes a new surface (under the inclusion) of the base alloy, which is more active than the surface covered with metallic oxides, leading to an abrupt decrease in the open circuit potential. This surface is also immediately oxidized to form metallic oxides, and the open circuit potential increases again, explaining potential discontinuity (points A and B in Fig. 1). The increase of the steel open circuit potential probably begins after the total dissolution of inclusions present at the examined electrode surface, and is due to oxidation of the alloy, with the formation of a more homogeneous oxide film.

It is well known that MnS is an electronic conductor, and is polarized to the same corrosion potential as the steel when exposed to different solutions.[1] At potentials between –0.197 V and 0.01 V(Ag/AgCl/$KCl_{sat.}$), the sulphide has no thermodynamic stability and tends to dissolve.[1] The dissolution rate of MnS inclusions, as a function of the corrosion potentials of 304 stainless steel, was confirmed by means of surface analyses.[1,30] In addition, the dissolution of the inclusions probably begins at the initial immersion times at open circuit potential, as observed by Lampner[31] for 304 stainless steel in 0.1 mol L^{-1} NaCl aqueous solution. Also, it is important to note that the 316 stainless steel showed an open circuit potential around +0.3 (V/Ag/AgCl/$KCl_{sat.}$) at *p*H < 3 in 3% NaCl aqueous solution.[1] In the present work, for chloride concentrations studied in acidic medium the values of E_{corr} (obtained from polarization curves and open circuit potentials) were between 0.20 and 0.38 V, increasing this potential as the Cl^- concentration decreased. On the other hand, the sulphides dissolution might be affected by the ethanol presence leading to more positive potentials as observed in the case of steel corrosion potential in solution containing ethanol compared to that in aqueous solution. In this case, it was noticed changes in the potential as high as 0.4 V.

For the stainless steel used, in the presence of the water/ethanol mixture the inclusions dissolution potential (the potential associated with the discontinuity) appear at around 0.22 and 0.32 V/(Ag/AgCl/$KCl_{sat.}$ for 0.006 wt % and 6×10^{-5} wt % NaCl, respectively. The higher potential values compared to the range from −0.197 to 0.01 V/Ag/AgCl/$KCl_{sat.}$,[1] are possibly due to the inhibition of inclusion dissolution related by the presence of ethanol in the mixture. The polarization curves obtained for 316L stainless steel, in aqueous solution and in a mixture of 65 wt % ethanol, 35 wt % water, both containing 1 wt % H_2SO_4 and 0.35 wt % NaCl, showed that the presence of ethanol caused inhibition of steel dissolution, as evidenced by an increase in E_{corr}.[12] Additionally, Elsener et al.,[19] who also showed that in solutions containing the mixture of ethanol/water/0.5 mol L^{-1} HCl, with different water concentrations, 304 stainless steel presented an active-passive transition that was strongly dependent on the solution water content.

The discontinuity in the E_{OC} curve for the steel in solution containing 0.006 wt % NaCl appears after shorter time intervals, and the potential is lower than that obtained in the solution with 6×10^{-5} wt % NaCl. This may be pertaining to the acceleration of inclusions dissolution owing to the increased NaCl concentration. To support this hypothesis, the work of Webb and Alkire,[32,33] concerning pitting initiation in sulphide inclusions present in stainless steel, showed that an increased NaCl concentration favoured the dissolution of MnS inclusions in the steel.

In order to confirm the dissolution of MnS inclusions associated to the discontinuity noticed in E-t profiles, SEM images (Fig. 2) of

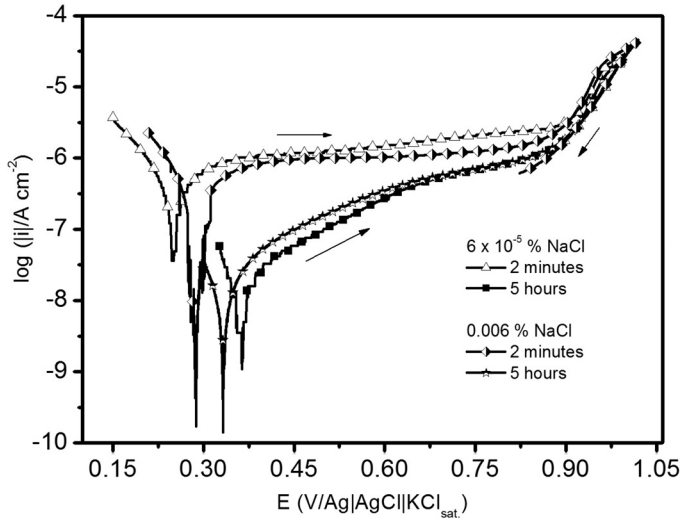

Figure 3. Polarization curves obtained for 316L stainless steel in 65 wt % ethanol, 35 wt % water, 1 wt % H_2SO_4 solution containing different NaCl concentrations, after immersion for 2 min and 5 h at open circuit and polarized up to the transpassive region, at 0.167 mV s^{-1} and 25°C.

Downloaded on 2013-07-18 to IP 186.217.234.138 address. Redistribution subject to ECS license or copyright; see ecsdl.org/site/terms_use

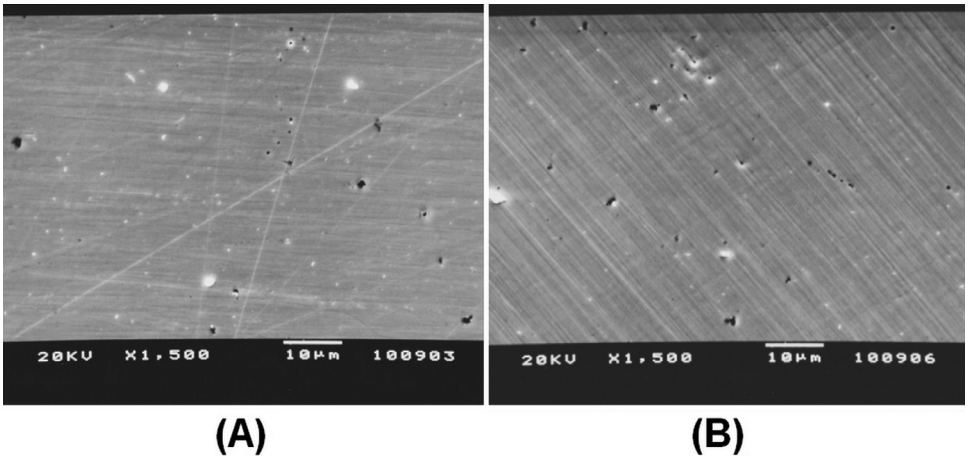

Figure 4. SEM images of 316L stainless steel exposed for 5 h at open circuit and polarized up to 0.50 V(Ag/AgCl) (A) and 0.70 V(Ag/AgCl) (B) in 65 wt % ethanol, 35 wt % water, 1 wt % H_2SO_4 solution containing 6×10^{-5} wt % NaCl, at 25°C.

polished stainless steel were taken after 20 and 30 min of immersion in the ethanolic solutions for 0.006 wt % and 6×10^{-5} wt % NaCl, respectively. It is seen the presence of small pits and the initio of inclusions dissolution (image A, 20 min immersion). As the immersion time increases the attack to produce both pits and inclusions dissolution also increases in number and size. Inclusions dissolution generates regular form while pits are normally observed as irregular ones (Image B).

Figure 3 displays the polarization curve for 316L stainless steel in the ethanolic aqueous solution containing different chloride concentrations, recorded after 2 min and 5 h immersion, at 25°C. For 6×10^{-5} wt % NaCl, the corrosion and transpassivation potentials were 0.37 and 0.9 V(Ag/AgCl/$KCl_{sat.}$), respectively. For potentials higher than the corrosion potential, increase of current density is due to oxidation of the steel, and was associated with the creation of defects in the passive oxide film, which had been previously formed under open circuit conditions. As in the potential range of the polarization curve no oxygen evolution was observed, the potential interval of polarization curves for low chloride concentrations was extended up to 2 V/Ag/AgCl/$KCl_{sat.}$ (Figure not shown). No oxygen evolution was observed and therefore it was concluded that the transpassivation region (about 0.9–2.0 V/Ag/AgCl/$KCl_{sat.}$) is not affected by oxygen reaction. For instance, Song[34] showed that the transpassive region for 304 stainless steel begins at 0.9 V/SCE in 0.5 mol L^{-1} H_2SO_4 aqueous solution, and the oxygen evolution was only observed at around +1.5 V/SCE. In 0.5 mol L^{-1} Na_2SO_4 aqueous solution the transpassive potential was +0.5 V/SCE and oxygen evolution was noticed at

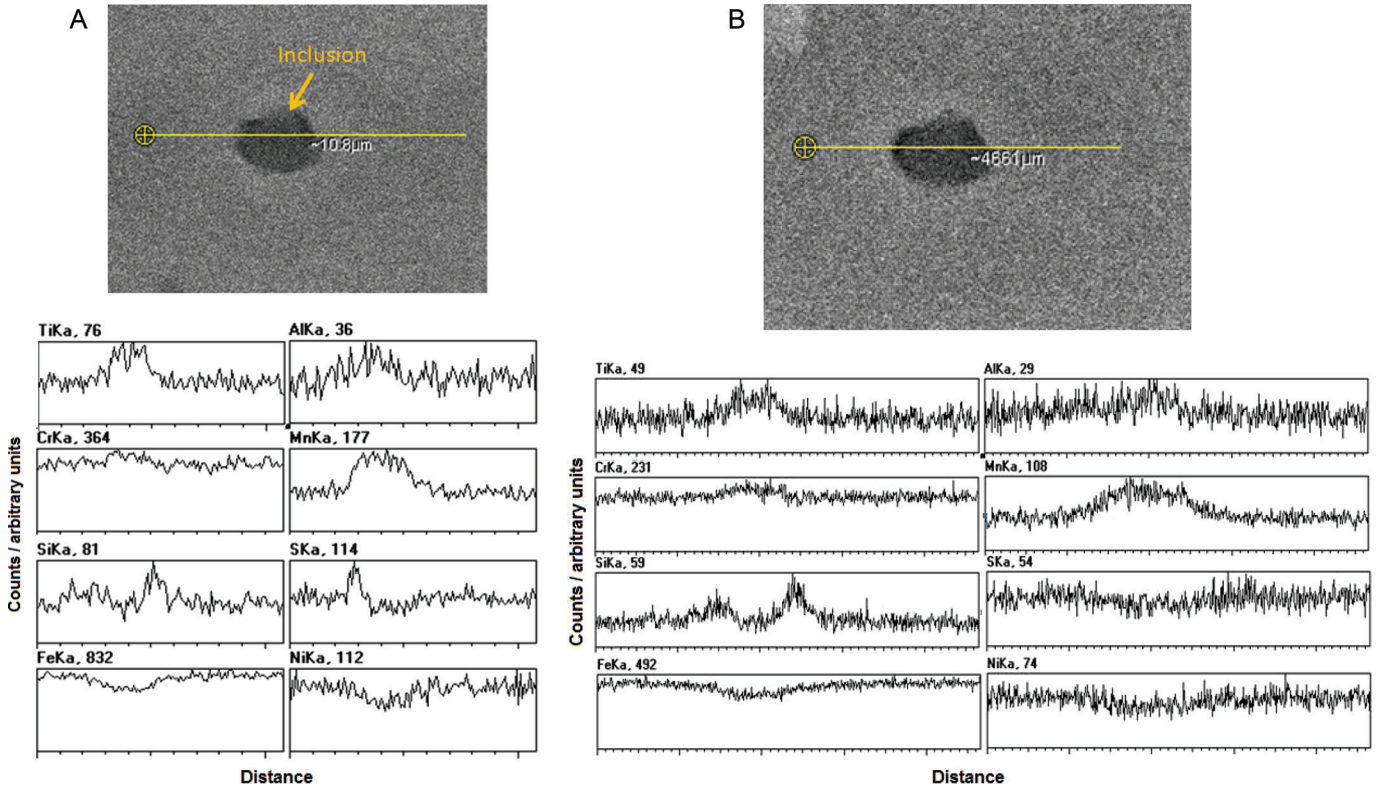

Figure 5. (Color online) SEM-FEG images and EDS line scan microanalysis of elements Cr, Si, Fe, Ti, Al, Mn, S, and Ni recorded for stainless steel before (polished stainless steel) (A) and after (B) of the polarization (see along lines direction: from left to right).

Downloaded on 2013-07-18 to IP 186.217.234.138 address. Redistribution subject to ECS license or copyright; see ecsdl.org/site/terms_use

Table III. Parameters for the circuit elements obtained from the adjustment of their responses to the experimental data of impedance for 316L stainless steel after 2 and 5 h of exposure to 65 wt % ethanol, 35 wt % water, 1 wt % H_2SO_4 solution containing 6×10^{-5} wt % NaCl, at 25°C, applying the open circuit potential. The % errors associated with each estimative are given in parentheses.

Immersion time (h)	E_{dc} (*) (mV)	R_s (Ω cm^2)	R_f (MΩ cm^2)	Q_f (μF cm^{-2} s^{n-1})	n	χ^2	L (nm)
2	363	96 (0.49%)	0.3 (1.70 %)	47.6 (0.53 %)	0.94 (0.17 %)	7.8×10^{-4}	0.2
5	385	107 (0.41%)	0.5 (1.55 %)	38.2 (0.42 %)	0.94 (0.14 %)	5.3×10^{-4}	0.3

(*) The EIS measurements were obtained polarizing the electrode on its respective open circuit potential.

about +1.0 V/SCE. Hence, we believe that the presence of ethanol is responsible for the shifting of the oxygen evolution potential to more positive values.

Figure 4 shows SEM images of steel, potentiodynamically polarized up to both 0.50 and 0.70 V(Ag/AgCl/KCl$_{sat.}$). The cavities observed on the surface were associated with the dissolution of MnS inclusions.

Figures 5A and 5B display the SEM images of 316L stainless steel before polarization (after mechanical polishing) and after polarization, respectively. Before polarization the presence of an inclusion which contains the elements Mn, S, Al, Si and an excess of Ti is observed. The presence of Mn and S along with other elements shows that the inclusion is composed of a mixture of MnS and Ti, Al and Si compounds. Stainless steels, such as type 316, contain a variety of inclusions in the form of oxides, silicates, aluminates, and sulphides. These are often present as mixed species, where the sulphides form shells around the oxides, silicates and aluminates.[1,30] Following to the steel polarization at +0.5 V(Ag/AgCl/KCl$_{sat.}$), in the region associated to the inclusion presence, was mainly noticed the decrease of Mn and S content.

For 6×10^{-3} wt % NaCl higher E_{corr} values were measured after 5 h than after 2 min immersion, suggesting that a thicker oxide film was formed after a longer immersion time. After 5 h at open circuit, the E_{corr} value (Fig. 4) was in agreement with that observed in Fig. 1. In other words, the higher is the chloride concentration, the smaller the corrosion potential. However, this is not true when the rest time was 2 min. In this case, the higher the chloride concentration the higher the corrosion potential, which is related to the electrode pre-treatment prior to exposure to the solution. After polishing the material, the instantaneous formation of an oxide layer may occur before exposure to the solution, due to the presence of oxygen in air. Under these conditions, the oxide thickness cannot be controlled. Hence, in the first 2 min, the value of the open circuit potential resulting from thickening of the oxide formed on the steel may be determined by the film thickness and defects in the oxide formed in air. For longer exposure times (5 h at open circuit), a greater film thickening occurred compared to that obtained up to 2 min (see Table III).

For the sample immersed for 2 min, the current densities in the passive region (~0.3 to ~0.9 V(Ag/AgCl/KCl$_{sat.}$)) were practically constant only for higher chloride concentrations, and higher than those obtained after 5 h immersion. This suggests that the oxide film formed under open circuit conditions was thicker for the sample immersed for 5 h, which explains the lower anodic current densities observed during its polarization. Additionally, for the steel exposed for 2 min at open circuit, with polarization, the constant current density values in the potential region from 0.3 to 0.9 V(Ag/AgCl/KCl$_{sat.}$) indicate that the film growth starts once the electrical field exceeds a critical value, which is equivalent to the film thickness formed under open circuit conditions for 2 min. In general, the drop of the applied potential takes place in the metal/film interface, own film, and film/solution interface, and the potentials shift to more positives values are only associated to the film thickening once the main part of the potential drop occurs in the oxide film. Thus, in the passivation region during the anodic polarization there is no influence of the metal/oxide and oxide/solution interfaces (e.g., the double layer). In this case, the film thickness increases linearly with potential, and consequently the electrical field (~10^6–10^7 V cm^{-1}) and the current density remain constant during the process. Thus, as the potential increases, both the charge transfer in the interfaces and the film thickness increase, due to the migration of cations (M^{n+}) from the metal/film interface to the film/solution interface, and migration of anions (O^{2-}) in the opposite direction.[35–37]

For the steel exposed at open circuit potential for 5 h, the polarization curve profile may be associated with greater thickness, degree of surface roughness and/or ageing of the film that was formed during exposure for a long period. Blackwood and Peter,[38] studying the stability and rupture at open circuit of a passive oxide film on titanium, showed that some degree of surface roughness and structural changes of the film (film ageing) might, with film reconstruction by means of anodic polarization, lead to a slow current increase as a function of the applied potential. With respect to film ageing, this process may lead to a more dense crystalline structure and, consequently, increase the height of the barrier to ion migration.

In order to determine the minimum NaCl concentration needed for pitting formation at 25°C, polarization curves for 316L stainless steel were obtained using solutions containing different NaCl concentrations (Fig. 6). E_{corr} values were between 0.20 and 0.30 V(Ag/AgCl/KCl$_{sat.}$), indicating little influence of salt concentration. Conversely, in the transpassive region a very different I-E profile was obtained in the solution containing 0.58 wt % NaCl. At around 0.95 V(Ag/AgCl/KCl$_{sat.}$), the current density abruptly increased by about 1 order of magnitude, with respect to the passive current, and remained almost constant up to 0.5 V(Ag/AgCl/KCl$_{sat.}$) in the reverse scan, suggesting a strong localized corrosion process. It is well known that the presence of inclusions in 316L stainless steel is one of the

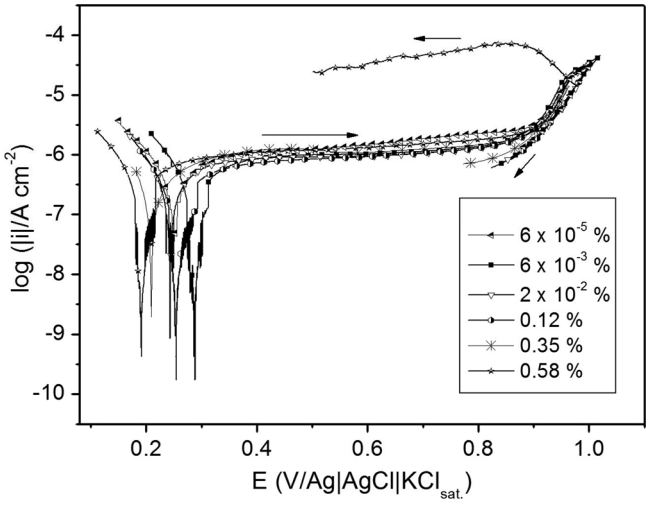

Figure 6. Polarization curves for 316L stainless steel obtained in 65 wt % ethanol, 35 wt % water, 1 wt % H_2SO_4 solution containing different NaCl concentrations, at 0.167 mV s^{-1} and 25°C.

Downloaded on 2013-07-18 to IP 186.217.234.138 address. Redistribution subject to ECS license or copyright; see ecsdl.org/site/terms_use

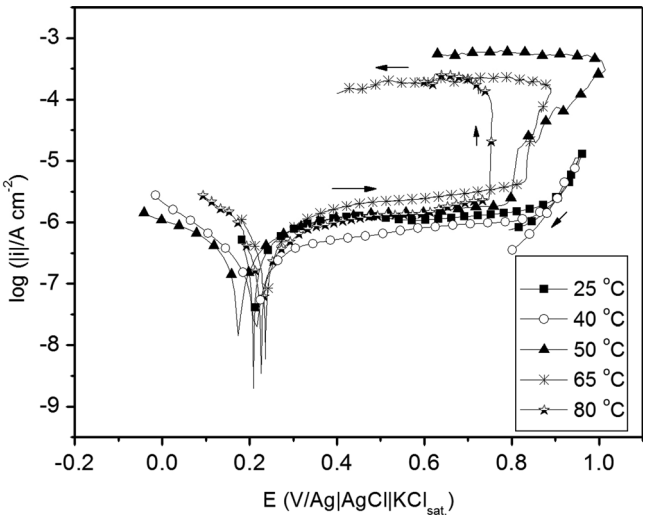

Figure 7. Polarization curves for 316L stainless steel obtained in 65 wt % ethanol, 35 wt % water, 1 wt% H_2SO_4 solution containing 0.35 wt % NaCl, at different temperatures and at 0.167 mV/s.

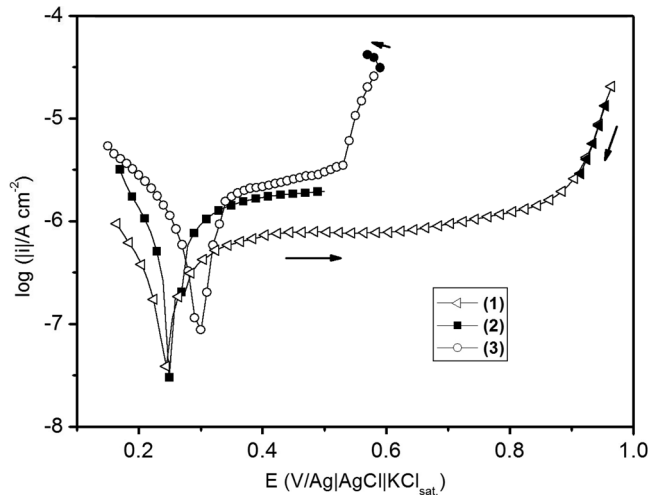

Figure 8. Polarization curves for 316L stainless steel obtained in 65 wt % ethanol, 35 wt % water, 1 wt % H_2SO_4 solution containing 0.35 wt % NaCl, up to different potentials and/or temperatures: (1) +0.914 V(Ag/AgCl/KCl$_{sat.}$) (transpassive region) at 40°C; (2) +0.500 V(Ag/AgCl/KCl$_{sat.}$) (imperfect passive region) at 65°C; (3) +0.570 V(Ag/AgCl/KCl$_{sat.}$) (pitting corrosion region) at 65°C. $v = 0.167$ mV s^{-1}.

main reasons for initiation of pitting corrosion.[1,9,10,30,39,40] For lower chloride concentrations (≤0.35 wt % NaCl), the current density decreased after switching the potential at 1 V(Ag/AgCl/KCl$_{sat.}$), indicating no pitting formation at a temperature of 25°C or lower.

Since no pitting formation was detected at 25°C in the presence of 0.35 wt % chloride, the temperature of the solution was increased in order to determine the CPT.

Figure 7 shows polarization curves for 316L in 0.35 wt % NaCl at different temperatures from 25 to 80°C. At 25 and 40°C, transpassivation was observed for potentials higher than +0.9 V(Ag/AgCl/KCl$_{sat.}$), and in the reverse scan the current was similar to that measured during the direct scan. At temperatures ≥50°C, an abrupt increase in the current was observed at certain potentials, all less positive than the transpassive potential (around +0.9 V(Ag/AgCl/KCl$_{sat.}$)), indicating that pitting was occurring. When this feature was observed, the potential scan was reversed, and the current measured was higher than that measured in the direct sweep, confirming that the active area had increased. For each temperature ≤40°C, and ≤0.35 wt % NaCl, at least five polarization curves were recorded at different regions of the sample to test whether pit formation was occurring. For chloride concentrations below 0.35 wt % and temperatures ≤25°C, no pitting corrosion was observed, even when different regions of the sample were analyzed. Thus, under these conditions, the CPT ranged from 40 to 50°C.

Figure 8 shows polarization curves for samples treated up to the transpassive region at 40°C (curve 1), and up to the potential regions corresponding to imperfect passivity[41] or metastable pits (curve 2), and stable pit formation (curve 3), both at 65°C. To ensure that

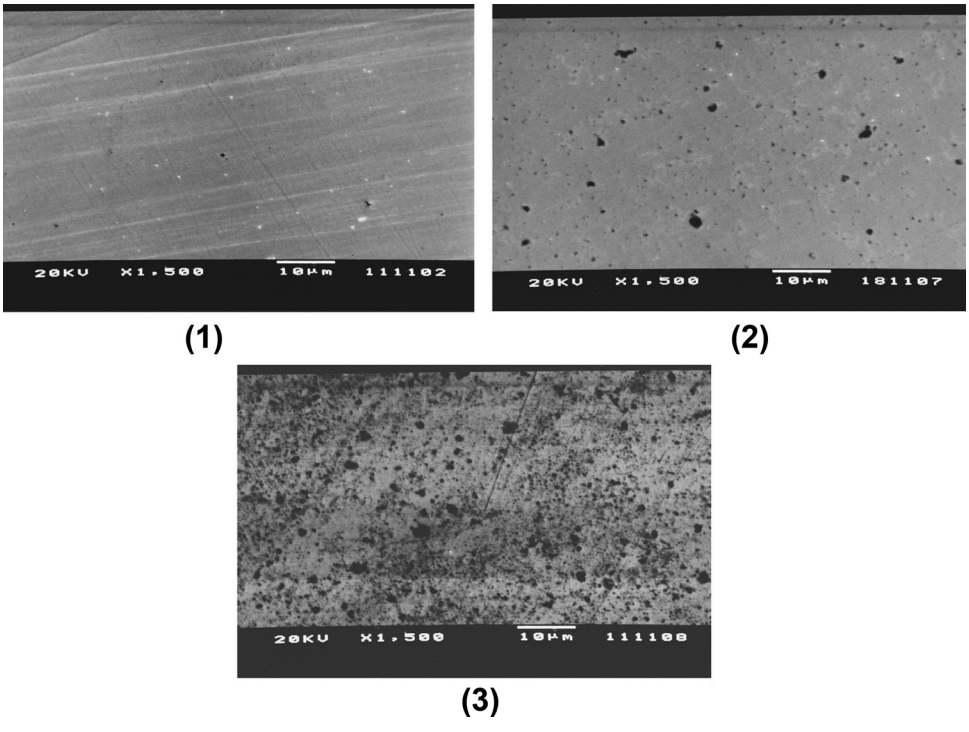

Figure 9. SEM micrographs of 316L stainless steel after polarizing in 65 wt % ethanol, 35 wt % water, 1 wt % H_2SO_4 solution containing 0.35 wt % NaCl, up to different potentials and/or temperatures: (1) +0.914 V(Ag/AgCl/KCl$_{sat.}$) (transpassive region) at 40°C; (2) +0.500 V(Ag/AgCl/KCl$_{sat.}$) (imperfect passive region) at 65°C; (3) +0.570 V(Ag/AgCl/KCl$_{sat.}$) (pitting corrosion region) at 65°C.

Downloaded on 2013-07-18 to IP 186.217.234.138 address. Redistribution subject to ECS license or copyright; see ecsdl.org/site/terms_use

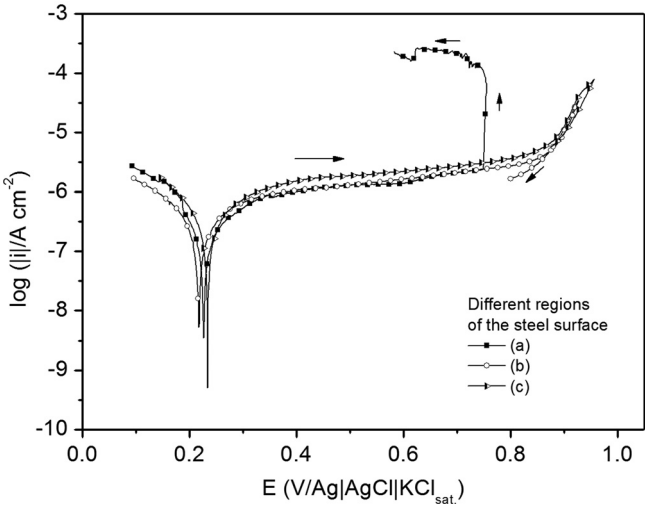

Figure 10. Polarization curves for 316L stainless steel in 65 wt % ethanol, 35 wt %water, 1 wt % H_2SO_4 solution containing 0.35 wt % NaCl, at 80°C and 0.167 mV/s.

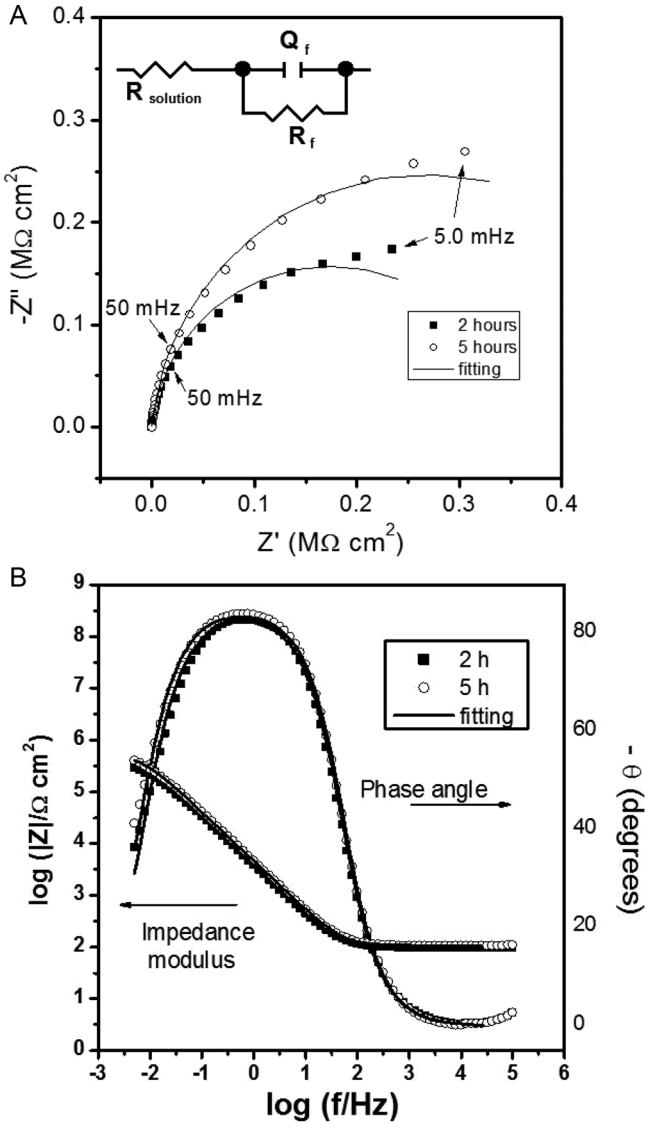

Figure 11. Experimental (symbol) and fitting (line) complex plane (a) and Bode (b) plots for 316L stainless steel recorded after 2 and 5 h of exposure to 65 wt % ethanol, 35 wt % water, 1 wt % H_2SO_4 solution containing 6×10^{-5} wt % NaCl, at 25°C, applying the open circuit potential.

metastable pitting formation occurred at the potential below the pitting potential, after attainment of the specific pitting potential, the current was reversed up to the repassivation potential. Metastable pit formation takes place in the potential region between the repassivation and pitting potentials.[6] Based on this concept, the results shown in Figs. 7 and 8 confirmed the formation of metastable pits on the steel at +0.5 V(Ag/AgCl/KCl$_{sat.}$) (curve 2). In Fig. 7, the polarization curve at 65°C suggests that reversing the potential, the current tends to diminish to potentials smaller than +0.4 V(Ag/AgCl/KCl$_{sat.}$). Therefore, the repassivation potential is smaller than +0.5 V(Ag/AgCl/KCl$_{sat.}$) which is located in the region between the repassivation and pitting potentials.

SEM micrographs of these regions are shown in Fig. 9. Metastable pitting occurs prior to the potential required for pitting. According to Frankel[6] metastable pits are pits that initiate and grow for a limited period before repassivating, and that can form at potentials far below the pitting potential (which is associated with the initiation of stable pits). Before the onset of stable pitting, metastable pits form at potentials below the pitting potential. At the transpassive region, the main feature was a higher inclusions dissolution density, without growth of pitting, while at the localized corrosion region, where stable pits start growing, a high density of pits and surface degradation were observed.

Figure 10 shows potentiodynamic curves recorded at 80°C at three different regions of the stainless steel sample surface, with only one showing pitting corrosion, characterized by current density increase in the reverse scan. It seems that the occurrence of localized corrosion is strongly dependent on the sample region chosen for analysis, in addition to the chloride concentration and temperature. This result also suggests that the steel surface does not have a uniform distribution of inclusions. Hence, it can be supposed that some of the regions randomly chosen on the steel surface could have possessed inclusions that led to pitting initiation.

Electrochemical impedance spectroscopy analysis.— Figure 11 shows experimental and adjusting complex plane and Bode plots for stainless steel immersed in the electrolyte containing 6×10^{-5} wt % NaCl, recorded applying the open circuit potential after 2 and 5 h immersion, and with the electrical equivalent circuit (EEC) used for fitting experimental data. For both immersion times only one time constant was observed, centred at around 0.3 Hz, with a markedly capacitive behaviour and maximum phase angle of −85°. According to Park et al.,[42] a single semicircle described the impedance spectra obtained for 316L stainless steel in a solution containing 0.5 mol L^{-1} NaCl and 0.5 mol L^{-1} $NaHCO_3$. The complex plane plots shown by passive metals correspond to the charge transfer reaction by means of ionic migration through the passive oxide film.[43] It can be noticed from the complex plane and Bode plots that the sample immersed for 5 h was more resistant than that exposed for 2 h. This difference was due to the increase of film thickness as a function of immersion time, since the film thickness after 5 h immersion was probably thicker than that obtained after 2 h, due to the injection of cations (Fe^{2+}, Cr^{3+}, Ni^{2+} and so on) onto the metal/oxide interface, and anions (O^{2-}) onto the solution/oxide interface (Table II). El Kader et al.[44] studied the variation of E_{oc} of a previously polished titanium electrode, as a function of time in different electrolytes, up to attainment of the steady state potential. In all cases, immediately after electrode immersion the E_{oc} changed to more positive values, indicating the occurrence of an increase of the oxide film thickness.[45,46] The film thickness increased as a function of time, up to attainment of the steady state potential.

The electrical equivalent circuit (EEC, see Fig. 11a) fitted the experimental data for the different immersion times, applying the sinusoidal perturbation on the open circuit potential, using the non-linear

Downloaded on 2013-07-18 to IP 186.217.234.138 address. Redistribution subject to ECS license or copyright; see ecsdl.org/site/terms_use

least squares method by means of software developed by Boukamp.[47] The heterogeneity of the studied systems leads to non-ideal capacitive responses, so the so-called constant phase element substituted the capacitance.[43] Figures 11a and 11b also show the results of impedance data fitting. The sum of square deviations, χ^2 around 10^{-4}, the low errors (%) associated with estimation of all the parameters (Table III), and the good matching between the fitted and the experimental diagrams (see continuous lines in Figs. 11a and 11b) indicate the adequacy of the proposed EEC. This circuit is similar to the one proposed by Wallinder et al.,[48] studying 304L stainless steel in aqueous solution containing 0.05 mol L^{-1} H_2SO_4 and 0.05 mol L^{-1} NaCl, after exposing the sample for 90 min at open circuit and polarizing the electrode at open circuit potential. Park et al.[42] also obtained similar results for 316L stainless steel in solution containing 0.5 mol L^{-1} NaCl and 0.5 mol L^{-1} $NaHCO_3$, applying different anodic potentials.

In ethanolic aqueous solution containing 6×10^{-5} wt % NaCl, the CPE values of steel decreased as a function of exposure time, which is another indication of the formation of a new phase, since the film thickness increased as the CPE values decreased, and the resistivity of the oxide film also increased (Table III). Similar behaviour of the metallic oxide parameters (resistance and CPE) were also observed by Patrito et al.[49] and Patrito and Macagno,[50] studying Zr in different electrolytes (H_2SO_4, NaOH, HNO_3 and H_3PO_4). The n values are greater than 0.9, suggesting near-capacitor behaviour.

Finally, estimation of the film thickness (Table III) was performed, taking into account that these films presented similar behaviour to a capacitor, using the equation[51,52]

$$L = \frac{\varepsilon\varepsilon_0}{C}$$

where L is the film thickness, ε is the dielectric constant of the passive film [ε = 12 (Refs. 51 and 52)], ε_o is the vacuum permittivity (8.854×10^{-14} F/cm) and C is the value of the capacitance of the film. The passive film thickness values obtained are realistic, and similar to those determined previously using different techniques.[53,54]

Conclusions

The E_{OC} values for 316L stainless steel immersed in 65 wt % ethanol, 35 wt %water, 1 wt % H_2SO_4 solution containing different NaCl concentrations were close to 0.4 V($Ag/AgCl/KCl_{sat.}$) after 5 h in a solution containing 6×10^{-5} wt % NaCl, and 0.35 V($Ag/AgCl/KCl_{sat.}$) after 2 h in a solution containing 0.006 wt % NaCl. The increase of E_{OC} to more positive values indicated formation of oxide with protective properties on the metallic surface. The solution containing a higher NaCl concentration presented smaller E_{OC} values. The increase of NaCl concentration might induce rupture and/or increase the film conductivity, provoking localized attack. The dissolution of superficial MnS inclusions seemed to be responsible for the discontinuity in both E_{OC} *vs*. time curves, which occurred after close to 15 min immersion in the solution containing 0.006 wt % NaCl, and after 45 min in the solution containing 6×10^{-5} wt % NaCl. From the complex plane and Bode plots, it appeared that the sample immersed for 5 h in a solution containing 6×10^{-5} wt % NaCl was more resistant than that exposed for 2 h. The same electrical equivalent circuit was used to fit the data obtained for stainless steel immersed in the electrolyte for 5 and 2 h.

In conclusion, the conditions necessary for use of 316L stainless steel in ethanol plant reservoirs are dependent on the chloride concentration and temperature. The minimum NaCl concentration for pitting formation and growth to occur was 0.58 wt % NaCl at 25°C. In 0.35 wt % NaCl, localized corrosion was observed at temperatures ≥50°C, and either metastable or stable pits were observed, depending on the potential.

Acknowledgments

The authors gratefully acknowledge financial support and scholarships from the Brazilian funding agencies FAPESP (proc. nº 2008/50579-7) and CNPq (proc. nº 300728/2007-7).

Fundunesp assisted in meeting the publication costs of this article.

References

1. A. J. Sedriks, *Corrosion of Stainless Steels*, John Wiley & Sons, Inc., New York (1996).
2. A. Kocijan, C. Donik, and M. Jenko, *Corros. Sci.*, **49**, 2083 (2007).
3. M. Kuczynska-Wydorska and J. Flis, *Corros. Sci.*, **50**, 523 (2008).
4. A. Pardo, M. C. Merino, A. E. Coy, F. Viejo, R. Arrabal, and E. Matykina, *Corros. Sci.*, **50**, 780 (2008).
5. D. A. Jones, *Principles and Prevention of Corrosion*, 2nd ed., Prentice-Hall, Englewood Cliffs, NJ (1996).
6. G. S. Frankel, *J. Electrochem. Soc.*, **145**, 2186 (1998).
7. J. R. Galvele, *Corros. Sci.*, **47**, 3053 (2005).
8. N. J. Laycock, M. H. Moayed, and R. C. Newman, *J. Electrochem. Soc.*, **145**, 2622 (1998).
9. V. Scotto, G. Ventura, and E. Traverso, *Corros. Sci.*, **19**, 237 (1979).
10. Z. Szklarska-Smialowska, *Corrosion (Houston)*, **28**, 388 (1972).
11. S. A. M. Refaey, F. Taha, and A. M. Abd El-Malak, *J. Electrochem. Sci.*, **1**, 80 (2006).
12. E. A. Ferreira, R. D. Noce, C. S. Fugivara, and A. V. Benedetti, Abstracts of the 61st Annual Meeting of the International Society of Electrochemistry, Nice, 2010.
13. P. L. Anna, *Corros. Sci.*, **25**, 43 (1985).
14. I. Sekine, M. Yuasa, and K. Kohara, *Corros. Sci.*, **31**, 579 (1990).
15. S. Tajima, S. Komatsu, and T. Momose, *Corros. Sci.*, **16**, 191 (1976).
16. E. Constantinescu and E. Heitz, *Corros. Sci.*, **16**, 857 (1976).
17. C. A Farina, G. Faita, and F. Olivani, *Corros. Sci.*, **18**, 465 (1978).
18. F. Bellucci, G. Capobianco, G. Faita, C. A. Farina, G. Farnia, F. Mazza, and S. Torchio, *Corros. Sci.*, **28**, 371 (1988).
19. B. Elsener, S. Virtanen, and H. Boehni, *Electrochim. Acta.*, **32**, 927 (1987).
20. V. K. Singh and V. B. Singh, *Corros. Sci.*, **28**, 385 (1988).
21. D. Shintani, T. Ishida, H. Izumi, T. Fukutsuka, Y. Matsuo, and Y. Sugie, *Corros. Sci.*, **50**, 2840 (2008).
22. D. Shintani, T. Ishida, and T. Fukutsuka, *Corrosion (Houston)*, **64**, 607 (2008).
23. C. E. V. Rossell, D. Lahr, A. G. P. Hilst, and M. R. L. V. Leal, *Int. Sugar. J.*, **107**, 192 (2005).
24. P. Brüesch, K. Müller, A. Atrens, and H. Neff, *Appl. Phys. A.*, **38**, 1 (1985).
25. J. M. A. El Kader and A. M. S. El Din, *Br. Corros. J.*, **14**, 40 (1979).
26. P. E. Manning and J. Duquette, *Corros. Sci.*, **20**, 597 (1980).
27. J.-L. Delplancke and R. Winand, *Electrochim. Acta.*, **33**, 1539 (1988).
28. S. Ferdjani, D. David, and G. Beranger, *J. Alloys Compd.*, **200**, 191 (1993).
29. E. A. Ferreira, N. T. C. Oliveira, S. R. Biaggio, P. A. P. Nascente, R. C. Rocha-Filho, and N. Bocchi, *Surf. Interface Anal.*, **38**, 417 (2006).
30. R. Ke and R. C. Alkire, *J. Electrochem. Soc.*, **139**, 1573 (1992).
31. D. Lampner, *In Situ Investigations of Corrosion Via SPM*, Application note, Agilent Technologies, Inc., USA, 5989-6895 EN (2007).
32. E. G. Webb and R.C. Alkire, *J. Electrochem. Soc.*, **149**, B272 (2002).
33. E. G. Webb and R. C. Alkire, *J. Electrochem. Soc.*, **149**, B280 (2002).
34. G. Song, *Corros. Sci.*, **47**, 1953 (2005).
35. Y. Chao, L. F. Lin, and D. D. Macdonald, *J. Electrochem. Soc.*, **128**, 1187 (1981).
36. E. X. Sun and W. B. Nowak, *Corros. Sci.* **43**, 1801 (2001).
37. D. J. Blackwood, L. M. Peter, and D. E. Williams, *Electrochim. Acta.*, **33**, 1143 (1988).
38. Q. Meng, G. S. Frankel, H. O. Colijn, and S. H. Goss, *Nature*, **424**, 389 (2003).
39. T. Suter, T. Peter, and H. Böhni, *Mater. Sci. Forum*, **192–194**, 25 (1995).
40. M. Pourbaix, *Corrosion (Houston)*, **26**, 431 (1970).
41. J.-J. Park, S.-I. Pyun, W.-J. Lee, and H.-P. Kim, *Corrosion (Houston)*, **55**, 380 (1999).
42. J. R. Macdonald, *Impedance Spectroscopy – Emphasizing solid materials and systems*, John Wiley & Sons, New York (1987).
43. J. M. A. EL Kader, F. M. A. EL Wahab, H. A. EL Shayed, and M. G. A. Khedr, *Br. Corros. J.*, **16**, 111 (1981).
44. J. M. A. El Kader and A. M. S. El Din, *Br. Corros. J.*, **14**, 40 (1979).
45. A. Mikó, J. W. Erning, H. Schlerkmann, and T. Mathiesen, *Electrochim. Acta.*, **54**, 7507 (2009).
46. B. A. Boukamp, *Solid State Ionics.*, **18**, 136 (1986).
47. D. Wallinder, J. Pan, C. Leygraf, and A. Delblanc-Bauer, *Corros. Sci.*, **42**, 1457 (2000).
48. E. M. Patrito, R. M. Torresi, E. P. M. Leiva, and V. A. Macagno, *J. Electrochem. Soc.*, **137**, 524 (1990).
49. E. M. Patrito and V. A. Macagno, *J. Electroanal. Chem.*, **375**, 203 (1994).
50. A. Fattah-Alhosseini, A. Saatchi, M. A. Golozar, and K. Raeissi, *J. Appl. Electrochem.*, **40**, 457 (2010).
51. G. Goodlet, S. Faty, S. Cardoso, P. P. Freitas, A. M. P. Simões, M. G. S. Ferreira, and M. D. Belo, *Corros. Sci.*, **46**, 1479 (2004).
52. I. Nicic and D. D. Macdonald, *J. Nucl. Mater.*, **379**, 54 (2008).
53. C.-O. A. Olsson and D. Landolt, *Electrochim. Acta.*, **48**, 1093 (2003).
54. D. Hamm, C.-O. A. Olsson, and D. Landolt, *Corros. Sci.*, **44**, 1009 (2002).

Downloaded on 2013-07-18 to IP 186.217.234.138 address. Redistribution subject to ECS license or copyright; see ecsdl.org/site/terms_use